

Modified Conjugate Quantum Natural Gradient

Mourad Halla

Deutsches Elektronen-Synchrotron DESY, Platanenallee 6, 15738 Zeuthen, Germany

January 2025

Abstract. The efficient optimization of variational quantum algorithms (VQAs) is critical for their successful application in quantum computing. The Quantum Natural Gradient (QNG) method, which leverages the geometry of quantum state space, has demonstrated improved convergence compared to standard gradient descent [Quantum 4, 269 (2020)]. In this work, we introduce the Modified Conjugate Quantum Natural Gradient (CQNG), an optimization algorithm that integrates QNG with principles from the nonlinear conjugate gradient method. Unlike QNG, which employs a fixed learning rate, CQNG dynamically adjusts hyperparameters at each step, enhancing both efficiency and flexibility. Numerical simulations show that CQNG achieves faster convergence than QNG across various optimization scenarios, even when strict conjugacy conditions are not always satisfied—hence the term “Modified Conjugate.” These results highlight CQNG as a promising optimization technique for improving the performance of VQAs.

1. Introduction

Quantum computing has emerged as a powerful paradigm for solving computational problems that surpass the capabilities of classical algorithms. One of the most promising approaches in this domain is *Variational Quantum Algorithms (VQAs)* [1, 2, 3], which have been widely studied for applications in quantum chemistry, materials science, and condensed matter physics. Among them, the *Variational Quantum Eigensolver (VQE)* [4] plays a crucial role in approximating ground-state energies of quantum systems, offering a hybrid quantum-classical optimization framework.

VQE leverages the flexibility of parameterized quantum circuits (ansätze), which are iteratively optimized to minimize an energy-based cost function. The optimization is performed using suitable optimizers, while quantum processors handle state preparation and measurement. This hybrid approach enables VQE to efficiently explore the solution space, making it particularly relevant for near-term noisy intermediate-scale quantum (NISQ) devices.

Optimization strategies are crucial for the efficiency of VQAs, as they determine both the convergence rate and the quality of the approximated solutions. Traditional methods, such as gradient descent (GD), are often insufficient to handle the complex characteristics of quantum optimization landscapes. These landscapes, characterized

by non-convexity, noise, and barren plateaus, require more advanced algorithms to accelerate convergence and enhance robustness.

One of the sophisticated optimizers, as an alternative to GD, is the Quantum Natural Gradient (QNG) algorithm [5], which leverages the geometry of the parameter space to enhance optimization in variational quantum algorithms. By utilizing the Fubini-Study metric or quantum Fisher information [6], QNG captures the local curvature of the quantum state manifold, aligning updates with the natural geometry to accelerate convergence and identify regions of high curvature early in the optimization process [8]. Extensions to QNG have improved its robustness, including adaptations for noisy and nonunitary circuits [9], stochastic techniques for approximating the quantum Fisher information matrix [10], the Quantum Random Natural Gradient [11], and the Quantum Natural Gradient with Geodesic Correction [12], making it a powerful optimizer for VQAs. In this work, we further extend QNG by integrating the nonlinear conjugate gradient method.

The *nonlinear conjugate gradient method* is a widely used optimization technique for tackling high-dimensional *nonlinear optimization problems* [13, 19]. At each iteration, it constructs new search directions by conjugating the residuals from previous steps, effectively forming a *Krylov subspace* [15]. This method is computationally efficient, requiring only the current gradient and the previous search direction, thereby reducing memory complexity. Building on these foundations, the *classical natural gradient* method [7] has been integrated with nonlinear conjugate gradient techniques by replacing the Euclidean gradient with the classical natural gradient [16]. Inspired by this approach, we extend these principles to the quantum domain, applying the nonlinear conjugate gradient method to the QNG framework. This integration aims to enhance convergence efficiency in variational quantum algorithms.

This manuscript is structured as follows: Section 2.1 provides an overview of QNG and VQE. In Section 2.2, we introduce CQNG as an extension of QNG. Section 3 presents numerical simulations demonstrating that CQNG accelerates convergence. Finally, Section 4 summarizes the key findings and discusses potential future extensions.

2. Theory

2.1. Quantum Natural Gradient and VQE

This section provides an overview of the VQE and its optimization strategies, focusing on noise-free variational quantum circuits. For a comprehensive review of VQAs, readers are referred to [1, 2, 3]. An in-depth discussion of QNG can be found in [5].

A typical circuit in VQAs is constructed as a sequence of unitary operations:

$$U_L(\boldsymbol{\theta}) = V_L(\boldsymbol{\theta}_L)W_L \cdots V_1(\boldsymbol{\theta}_1)W_1, \quad (1)$$

where $V_i(\boldsymbol{\theta}_i)$ are parameterized unitary operators, W_i are fixed unitaries, and $\boldsymbol{\theta} = (\boldsymbol{\theta}_1 \oplus \cdots \oplus \boldsymbol{\theta}_L) \in \mathbb{R}^d$ represents the concatenated parameter vector.

The objective of VQE is to find the ground state of the observable \hat{O} by minimizing a cost function, typically defined as the expectation value of \hat{O} with respect to the parameterized quantum state $|\psi(\boldsymbol{\theta})\rangle = U(\boldsymbol{\theta})|\psi_0\rangle$:

$$\mathcal{L}(\boldsymbol{\theta}) = \langle \psi(\boldsymbol{\theta}) | \hat{O} | \psi(\boldsymbol{\theta}) \rangle, \quad (2)$$

where $|\psi_0\rangle$ is the initial state. The minimization of $\mathcal{L}(\boldsymbol{\theta})$ over the parameter space $\boldsymbol{\theta}$ yields an approximation of the ground state energy and its corresponding eigenstate. Gradient descent achieves this by iteratively updating the parameters:

$$\boldsymbol{\theta}_{t+1} = \boldsymbol{\theta}_t - \eta \partial_j \mathcal{L}(\boldsymbol{\theta}_t), \quad (3)$$

where $\partial_j := \frac{\partial}{\partial \theta^j}$, $\eta > 0$ is the learning rate, and t denotes the iteration step. The gradient of the cost function $\partial_j \mathcal{L}(\boldsymbol{\theta}_t)$ can be calculated using the parameter-shift rule [21, 22, 23].

In standard Gradient Descent (3), parameter updates are performed in a flat Euclidean space, which does not accurately capture the curved geometry of the quantum state manifold. QNG addresses this limitation by incorporating the Riemannian gradient, $F^{ij} \partial_j \mathcal{L}(\boldsymbol{\theta}_t)$, into the update rule:

$$\boldsymbol{\theta}_{t+1} = \boldsymbol{\theta}_t - \eta g^{ij} \partial_j \mathcal{L}(\boldsymbol{\theta}_t), \quad (4)$$

where the Fubini-Study metric F_{ij} (with F^{ij} as its inverse) is defined as:

$$F_{ij} = \text{Re}(\langle \partial_i \psi | \partial_j \psi \rangle) - \langle \partial_i \psi | \psi \rangle \langle \psi | \partial_j \psi \rangle. \quad (5)$$

The QNG is a robust and effective optimizer; however, it incurs additional computational overhead due to the calculation of the metric. Specifically, evaluating the full Fubini-Study metric F_{ij} for a circuit with n parameters requires $O(n^2)$ function evaluations, making it computationally demanding for large-scale systems. To mitigate this, the block-diagonal approximation is employed, significantly reducing the complexity. The key idea involves defining subcircuits between layers l_1 and l_2 as:

$$U_{[l_1:l_2]} = V_{l_2} W_{l_2} \cdots V_{l_1} W_{l_1}, \quad (6)$$

and expressing the full circuit recursively as:

$$U_L(\boldsymbol{\theta}) = U_{(l:L]} V_l W_l U_{[1:l)}, \quad (7)$$

where $(l : L] = [l - 1 : L]$ and $[1 : l) = [1 : l - 1]$. The quantum state at the l -th layer is defined as:

$$\psi_l := U_{[1:l)} |0\rangle. \quad (8)$$

For each layer $l \in [L]$, Hermitian generator matrices K_i and K_j are defined such that:

$$\partial_i V_l(\boldsymbol{\theta}_l) = -i K_i V_l(\boldsymbol{\theta}_l), \quad (9)$$

$$\partial_j V_l(\boldsymbol{\theta}_l) = -i K_j V_l(\boldsymbol{\theta}_l), \quad (10)$$

where $[K_i, K_j] = 0$ for distinct parameters $i \neq j$. The block-diagonal approximation of the Fubini-Study metric F_{ij} for layer l is then given by:

$$F_{ij}^{(l)} = \langle \psi_l | K_i K_j | \psi_l \rangle - \langle \psi_l | K_i | \psi_l \rangle \langle \psi_l | K_j | \psi_l \rangle. \quad (11)$$

If we consider circuits composed of single-qubit Pauli rotations, expressed as:

$$V_l(\boldsymbol{\theta}) = \bigotimes_{k=1}^n R_{P_{l,k}}(\boldsymbol{\theta}_{l,k}), \quad R_{P_{l,k}}(\boldsymbol{\theta}_{l,k}) = \exp\left(-i \frac{\boldsymbol{\theta}_{l,k}}{2} P_{l,k}\right), \quad (12)$$

where $P_{l,k} \in \{\sigma_x, \sigma_y, \sigma_z\}$ are Pauli matrices acting on the k -th qubit. The Hermitian generator for parameter $\boldsymbol{\theta}_{l,k}$ is:

$$K_i = \frac{1}{2} \mathbb{1}^{[1,i]} \otimes P_{l,i} \otimes \mathbb{1}^{(i,n]}, \quad (13)$$

where $\mathbb{1}^{[1,i]} = \bigotimes_{1 \leq j < i} \mathbb{1}$ is the identity on preceding qubits. These generators satisfy $[K_i, K_j] = 0$ and $P_{l,i}^2 = \mathbb{1}$.

The metric block for layer l requires the evaluation of the quantum expectation value $\langle \psi_l | \hat{A} | \psi_l \rangle$, where \hat{A} is an operator from:

$$S_l = \{P_{l,i} \mid 1 \leq i \leq n\} \cup \{P_{l,i} P_{l,j} \mid 1 \leq i < j \leq n\}. \quad (14)$$

Since all operators in S_l commute, a single quantum measurement per layer is sufficient, reducing the required number of state preparations from $|S_l| = n(n+1)/2$.

To further improve optimization, in this work we propose integrating QNG with the nonlinear conjugate gradient method, which is discussed in the following section.

2.2. Modified Conjugate Quantum Natural Gradient

In this section, we extend the QNG algorithm by incorporating the nonlinear conjugate gradient method. For a modern review of conjugate gradient methods, we recommend the book [17].

The Modified Conjugate Quantum Natural Gradient (CQNG) extends the QNG algorithm (4) by incorporating principles from the nonlinear conjugate gradient method. The parameter update rule for CQNG, for steps $t \geq 0$, is defined as:

$$\boldsymbol{\theta}_{t+1} = \boldsymbol{\theta}_t + \alpha_t \mathbf{d}_t, \quad (15)$$

where the search directions $\mathbf{d}_t \in \mathbb{R}^n$ are computed as:

$$\mathbf{d}_t = \begin{cases} -F^{ij} \partial_j \mathcal{L}(\boldsymbol{\theta}_t) & \text{if } t = 0, \\ -F^{ij} \partial_j \mathcal{L}(\boldsymbol{\theta}_t) + \beta_t \mathbf{d}_{t-1} & \text{if } t \geq 1. \end{cases} \quad (16)$$

Here, $\alpha_t \in \mathbb{R}^+$ is the step size, F^{ij} denotes the inverse of the Fubini-Study metric, and $\beta_t \in \mathbb{R}$ is the conjugate coefficient that incorporates the influence of the previous search direction \mathbf{d}_{t-1} and ensures that the conjugacy condition is satisfied,

$$\mathbf{d}_t^T F_{ij} \mathbf{d}_{t-1} = 0. \quad (17)$$

Various formulas have been proposed for β_t , with the most well-known being those of Polak-Ribière [18], Fletcher-Reeves [19], and Dai-Yuan [20]. While these approaches are

widely used in classical optimization, their direct application in VQAs can introduce challenges, such as noise sensitivity in gradient estimations, stability issues due to the varying metric tensor, and increased computational costs.

A more practical approach that we adopt in this work for VQAs, inspired by classical deep networks, was proposed in [16]. Instead of using a predefined formula for β_t , we determine both α_t and β_t dynamically at each step by solving the following optimization problem:

$$(\alpha_t, \beta_t) = \arg \min_{\alpha, \beta} \mathcal{L}(\boldsymbol{\theta}_t + \alpha_t F^{ij} \partial_j \mathcal{L}(\boldsymbol{\theta}_t) + \beta_t \mathbf{d}_{t-1}), \quad (18)$$

This adaptive strategy enhances flexibility and robustness by jointly optimizing the step size and conjugate coefficient at each iteration, even when strict conjugacy conditions are not always satisfied. Due to this modification, we refer to the approach as the "Modified Conjugate". The main steps of the CQNG algorithm are summarized in Algorithm 1. In the next section, we present numerical simulations demonstrating its improved convergence performance compared to standard QNG.

Algorithm 1: Modified Conjugate Quantum Natural Gradient (CQNG)

Input: Problem Hamiltonian \hat{H} , Ansatz $|\psi(\boldsymbol{\theta})\rangle$, initial parameters $\boldsymbol{\theta}_0$, objective function $\mathcal{L}(\boldsymbol{\theta})$, maximum iterations T , regularization parameter λ , $\alpha_0 \in \mathbb{R}^+$, $\beta_0 \in \mathbb{R}$.

Output: Optimized parameters $\boldsymbol{\theta}_T$.

for $t = 0$ **to** $T - 1$ **do**

Compute the gradient: $\partial_j \mathcal{L}(\boldsymbol{\theta}_t)$;

Compute and regularize the metric tensor: $F_{ij} \leftarrow F_{ij}(\boldsymbol{\theta}_t) + \lambda \delta_{ij}$;

Compute the inverse metric tensor: F^{ij} ;

if $t = 0$ **then**

Set the search direction: $\mathbf{d}_t \leftarrow -F^{ij} \partial_j \mathcal{L}(\boldsymbol{\theta}_t)$;

else

Solve for optimal α_t and β_t using an optimizer with initial values α_0 and β_0 :

$$(\alpha_t, \beta_t) = \arg \min_{\alpha, \beta} \mathcal{L}(\boldsymbol{\theta}_t + \alpha \mathbf{d}_t + \beta \mathbf{d}_{t-1}).$$

if optimization fails then

Set default values: $\alpha_t \leftarrow \alpha_0$, $\beta_t \leftarrow 0$;

Update the search direction:

$$\mathbf{d}_t \leftarrow -F^{ij} \partial_j \mathcal{L}(\boldsymbol{\theta}_t) + \beta_t \mathbf{d}_{t-1}.$$

Update parameters:

$$\boldsymbol{\theta}_{t+1} \leftarrow \boldsymbol{\theta}_t + \alpha_t \mathbf{d}_t.$$

return $\boldsymbol{\theta}_T$;

3. Experimental Simulation

In this section, we present practical examples to demonstrate the accuracy and effectiveness of CQNG compared to GD and QNG. For the simulations, we employ two distinct approaches. Example 1, as a pedagogical example, consists of a two-qubit simulation of the hydrogen molecule (H_2), building on analytical results from our previous work [12]. In Example 2, we explore the Heisenberg model using the open-source software PennyLane [24], illustrating the scalability of our method. Additionally, for hyperparameter tuning in Example 2, we leverage the open-source software Optuna [25].

3.1. Example 1: Two-Qubit Simulation of the Hydrogen Molecule (H_2)

In this example, we determine the ground state energy of the hydrogen molecule (H_2) using a two-qubit VQE. The system is described by the following Hamiltonian:

$$H = h(\sigma_z \otimes I + I \otimes \sigma_z) + J\sigma_x \otimes \sigma_x, \quad (19)$$

where $h = 0.4$ and $J = 0.2$. Here, σ_z and σ_x are Pauli matrices acting on the qubits, with the parameters J and h controlling the interaction and magnetic field terms, respectively.

To approximate the ground state, we utilize a parameterized VQE ansatz designed to capture the system's entanglement and structure. This ansatz is given by:

$$|\psi\rangle = (CRY(\theta)_{q_0, q_1})(CRX(\theta)_{q_0, q_1})(R_y(2\theta_0) \otimes R_y(2\theta_1))|0\rangle \otimes |0\rangle \quad (20)$$

where $R_y(\theta) = e^{-i\theta\sigma_y/2}$ is a single-qubit rotation gate, and CRX, CRY are controlled rotation gates entangling the qubits.

The Fubini-Study metric, which governs the geometry of the parameter space, is computed as:

$$F = \begin{pmatrix} 1 & 0 & \cos(\theta_1) \sin(\theta_1) \\ 0 & 1 & -\cos(\theta_0) \sin(\theta_0) \\ \cos(\theta_1) \sin(\theta_1) & -\cos(\theta_0) \sin(\theta_0) & \frac{1}{2}(1 - \cos(2\theta_0) \cos(2\theta_1)) \end{pmatrix}. \quad (21)$$

To prevent singularities in F during parameter updates, a regularization term λ is added to its diagonal, ensuring numerical stability when computing the inverse metric, F^{-1} . The derivation of the inverse metric and additional details about this system are provided in [12].

With this setup, Fig. 1, Fig. 2, and Fig. 3 demonstrate that CQNG exhibits accelerated convergence compared to QNG and GD, reaching the target energy and high fidelity in fewer iterations. Furthermore, Fig. 2 shows that CQNG escapes plateaus earlier.

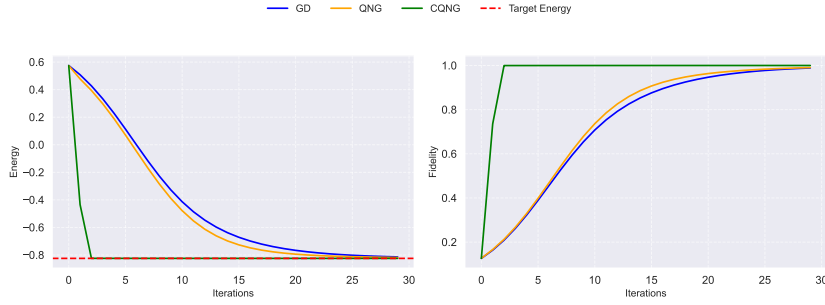


Figure 1. Energy convergence and fidelity to the ground state as a function of training iterations for GD, QNG, and CQNG optimizers. The initial parameters are set to $[-0.2, -0.2, 0]$, and a learning rate $\eta = 0.05$ is used for GD and QNG. The initial values $\beta_0 = 0.1$ and $\alpha_0 = 0.05$ are used for the COBYLA optimizer, which dynamically optimizes α_t and β_t at each step according to Eq. (18).

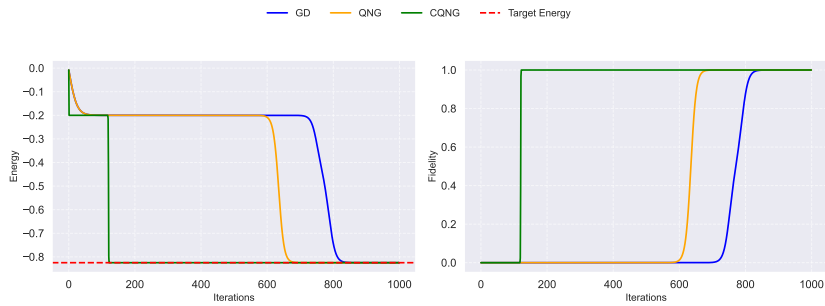


Figure 2. Same experimental conditions as in Fig. 1, but with the initial point set to $[\pi/2, \pi/2, 0]$.

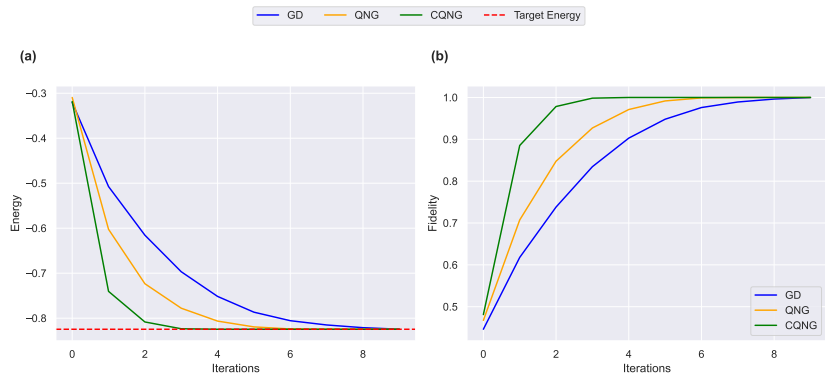


Figure 3. The average of 100 runs from different initial starting points. The hyperparameters, including the learning rate for GD and QNG, as well as the initial step size α_0 used in COBYLA for CQNG, are tuned using a grid search.

3.2. Example 2: Heisenberg Model

In this example, we use the VQE to find the ground state of the Heisenberg Hamiltonian.

The Heisenberg model is a fundamental quantum many-body system, widely studied for its rich physics and computational challenges. Its Hamiltonian for n spins is expressed as:

$$H = J \sum_{i=1}^{n-1} (\sigma_i^X \sigma_{i+1}^X + \sigma_i^Y \sigma_{i+1}^Y + \sigma_i^Z \sigma_{i+1}^Z) + h \sum_{i=1}^n \sigma_i^X, \quad (22)$$

where $\sigma_i^X, \sigma_i^Y, \sigma_i^Z$ are the Pauli operators acting on the i -th spin, J is the coupling constant, and h represents the strength of the external magnetic field. In this work, we consider the case where $J = -1$ and $h = -1$, making it a benchmark for testing quantum optimization methods.

To approximate the ground state of H , we employ the hardware-efficient **EfficientSU2** variational ansatz [26]. This ansatz combines layers of parameterized single-qubit R_Y and R_Z rotations with entangling CNOT gates, as illustrated in Fig. 4.

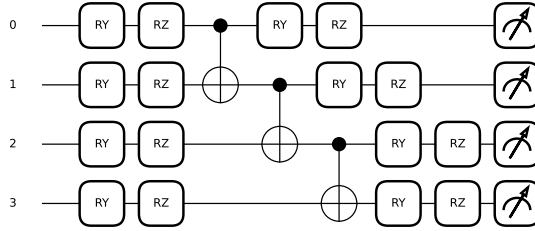


Figure 4. EfficientSU2 ansatz with two layers.

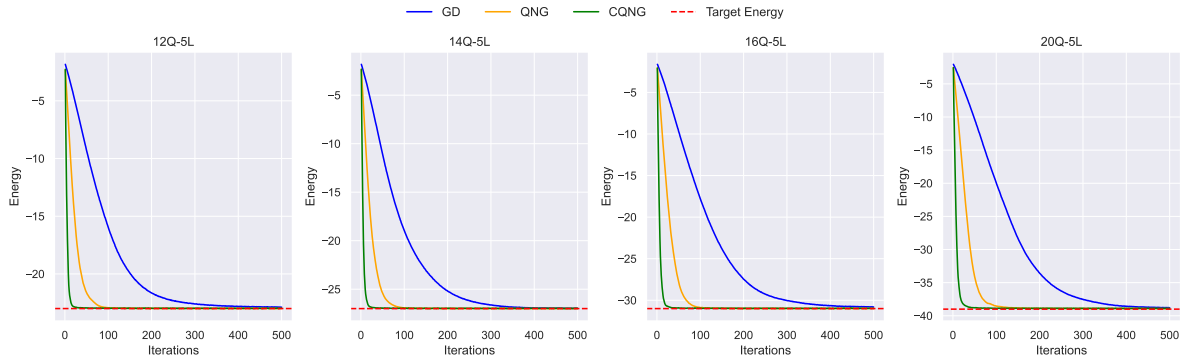


Figure 5. Average cost function value as a function of training iterations for GD, QNG, and CQNG, evaluated for 12, 14, 16, and 20 qubits with a fixed circuit depth of 5 layers. Each data point represents an average over 30 runs with different initial parameters. The number of measurement shots is set to 10024, with a learning rate of 0.01. The initial values $\beta_0 = 0.1$ and $\alpha_0 = 0.01$ are used for the COBYLA optimizer, which dynamically optimizes α_t and β_t at each step according to Eq. (18).

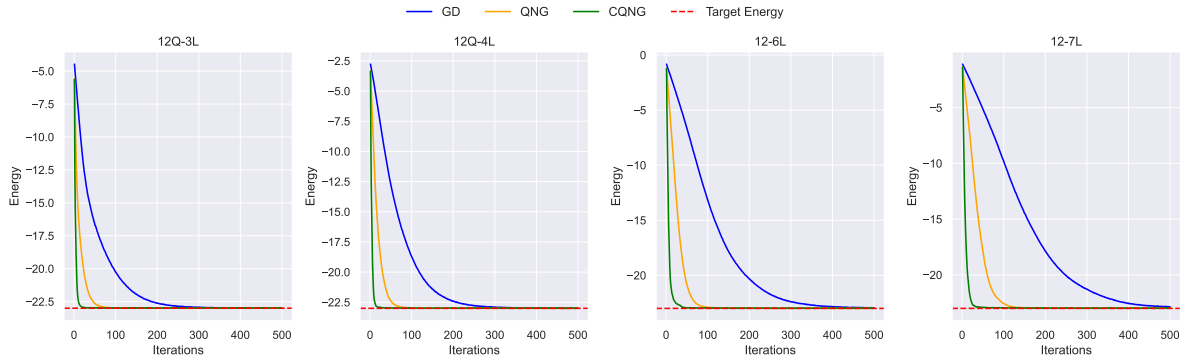


Figure 6. Same experimental conditions as in Fig. 5, but evaluated for circuit depths of 3, 4, 6, and 7 with a fixed qubit count of 12.

Like in Example 1, we benchmark the optimizers in different scenarios. In Figs. 5 and 6, we fix the learning rate, while in Figs. 7 and 8, we determine the optimal learning rates for GD and QNG, as well as the initial step size α_0 for COBYLA through hyperparameter tuning. As the figures illustrate, CQNG consistently outperforms GD and QNG in all scenarios by accelerating convergence and reducing the number of iterations needed to reach lower energy values.

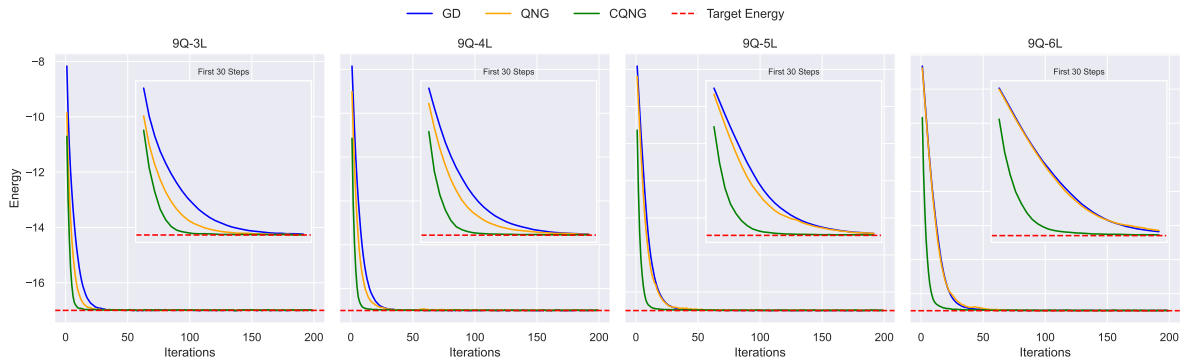


Figure 7. Average cost function value as a function of training iterations for GD, QNG, and CQNG, evaluated at circuit depths of 3, 4, 5, and 6 with a fixed qubit count of 9. Each data point represents an average over 30 runs with different initial parameters. The number of measurement shots is set to 10024. The learning rates for GD and QNG, as well as the initial step size α_0 in CQNG, are optimized using hyperparameter tuning.

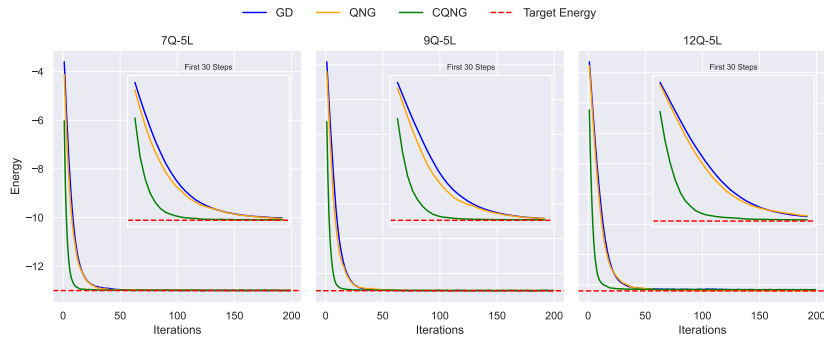


Figure 8. Same experimental conditions as in Fig. 7, but evaluated for 7, 9, and 12 qubits with a fixed circuit depth of 5 layers.

4. Conclusions and Outlook

We have introduced the *Modified Conjugate Quantum Natural Gradient (CQNG)*, an optimization algorithm that extends the *Quantum Natural Gradient (QNG)* by incorporating principles from the nonlinear conjugate gradient method. Unlike conventional QNG, which relies on a fixed learning rate, CQNG dynamically optimizes both the *step size* (α_t) and the *conjugate coefficient* (β_t) at each iteration.

Numerical simulations demonstrate that this adaptive approach significantly accelerates convergence compared to standard QNG, making CQNG a promising optimization method for variational quantum algorithms. However, the conjugacy condition, $\mathbf{d}_t^T \mathbf{F} \mathbf{d}_{t-1} = 0$, may not be strictly satisfied at every iteration of the optimization process. This motivates the term “*Modified Conjugate*” to reflect the practical adjustments made to improve performance while retaining the core advantages of conjugate gradient methods.

CQNG can be further developed in several directions. Similar to QNG, it can be adapted for noisy and nonunitary circuits following the approaches in [9]. The use of simultaneous perturbation stochastic approximation for the quantum Fisher information [10], as well as randomness-based methods [11], represents a promising avenue for our future research. Moreover, the methods introduced in CQNG could also be explored for applications in time-dependent quantum optimization problems, potentially extending its applicability to broader areas of quantum computing.

5. Acknowledgements

This work was supported by the Ministry of Science, Research, and Culture of the State of Brandenburg within the Centre for Quantum Technologies and Applications (CQTA) and by the German Ministry of Education and Research (BMBF) through the project NiQ.

Appendix A. Additional Experiments and Figures

In addition, we present the quantum state preparation for the ground state of the Heisenberg model with $J = h = -1$. Fig. A1 demonstrates that CQNG requires fewer quantum resources to achieve convergence compared to other methods.

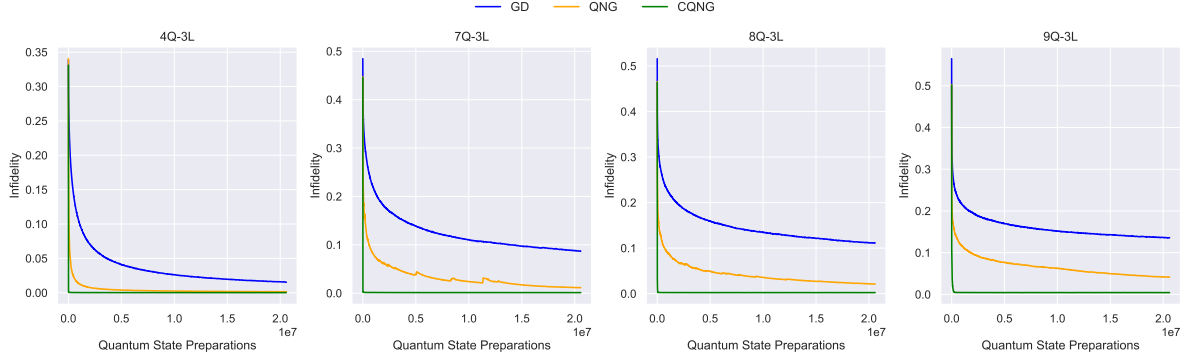


Figure A1. Average infidelity as a function of the number of quantum state preparations for GD, QNG, and CQNG, evaluated for 4, 7, 8, and 9 qubits with a fixed circuit depth of 3 layers. Each data point represents an average over 30 runs with different initial parameters. The number of measurement shots is set to 30024, with a learning rate of 0.01. The initial values $\beta_0 = 0.1$ and $\alpha_0 = 0.01$ are used for the COBYLA optimizer, which dynamically optimizes α_t and β_t at each step according to Eq. (18).

- [1] M. Cerezo, A. Arrasmith, R. Babbush, S. C. Benjamin, S. Endo, K. Fujii, et al., “Variational Quantum Algorithms,” *Nature Reviews Physics*, 3, 625-644 (2021). <https://doi.org/10.1038/s42254-021-00348-9>.
- [2] J. R. McClean, J. Romero, R. Babbush and A. Aspuru-Guzik, “The theory of variational hybrid quantum-classical algorithms,” *New Journal of Physics*, 18, 023023 (2016). <https://doi.org/10.1088/1367-2630/18/2/023023>.
- [3] K. Bharti, A. Cervera-Lierta, T. H. Kyaw, T. Haug, S. Alperin-Lea, A. Anand, et al., “Noisy intermediate-scale quantum algorithms,” *Reviews of Modern Physics*, 94, 015004 (2022). <https://doi.org/10.1103/RevModPhys.94.015004>.
- [4] A. Peruzzo, J. McClean, P. Shadbolt, M.-H. Yung, X.-Q. Zhou, P. J. Love, A. Aspuru-Guzik, and J. L. O’Brien, “A variational eigenvalue solver on a photonic quantum processor,” *Nature Communications* 5, 4213 (2014). <https://www.nature.com/articles/ncomms5213doi:10.1038/ncomms5213>.
- [5] J. Stokes, J. Izaac, N. Killoran, and G. Carleo, “Quantum Natural Gradient,” *Quantum* 4, 269 (2020). <https://doi.org/10.22331/q-2020-05-25-269>.
- [6] J. Jakob Meyer,, “Fisher Information in Noisy Intermediate-Scale Quantum Applications ,” *Quantum* 5, 539 (2021). <https://doi.org/10.22331/q-2021-09-09-539>.
- [7] S.-I. Amari, “Natural Gradient Works Efficiently in Learning,” *Neural Computation* 10 (2), 251-276 (1998). <https://doi.org/10.1162/089976698300017746>
- [8] A. Katabarwa, S. Sim, D. E. Koh, and P.-L. Dallaire-Demers, “Connecting geometry and performance of two-qubit parameterized quantum circuits,” *Quantum* 6, 782 (2022). <https://doi.org/10.22331/q-2022-08-23-782>.
- [9] B. Koczor and C. Benjani, “Quantum natural gradient generalized to noisy and nonunitary circuits,” *Phys. Rev. A* **106**, 062416 (2022). <https://doi.org/10.1103/PhysRevA.106.062416>.
- [10] J. Gacon, C. Zoufal, G. Carleo and S. Woerner, “Simultaneous Perturbation Stochastic Approximation of the Quantum Fisher Information ,” *Quantum* 5, 567 (2021). <https://doi.org/10.22331/q-2021-10-20-567>.
- [11] I. Kolotouros and P. Wallden, “Random Natural Gradient ,” *Quantum* 8, 1503 (2024). <https://doi.org/10.22331/q-2024-10-22-1503>.
- [12] M. Halla,, “Quantum Natural Gradient with Geodesic Corrections for Small Shallow Quantum Circuits ,” 2024. <https://doi.org/10.48550/arXiv.2409.03638>.
- [13] M. R. Hestenes and E. Stiefel, “Methods of Conjugate Gradients for Solving Linear Systems,” *Journal of Research of the National Bureau of Standards*, 49(6), 409-436 (1952). <https://doi.org/10.6028/jres.049.044>.
- [14] R. Fletcher and C. M. Reeves, “Function Minimization by Conjugate Gradients,” *The Computer Journal*, 7(2), 149-154 (1964). <https://doi.org/10.1093/comjnl/7.2.149>.
- [15] Y. Saad, “Iterative Methods for Sparse Linear Systems,” 2nd ed., SIAM, Philadelphia, 2003. <https://doi.org/10.1137/1.9780898718003>.
- [16] R. Pascanu and Y. Bengio, “Revisiting Natural Gradient for Deep Networks,” arXiv preprint arXiv:1301.3584 (2013). <https://arxiv.org/abs/1301.3584>.
- [17] N. Andrei, *Nonlinear Conjugate Gradient Methods for Unconstrained Optimization*, Springer, 2020. <https://doi.org/10.1007/978-3-030-42950-8>.
- [18] E. Polak and G. Ribière, “Note sur la convergence de méthodes de directions conjuguées,” *ESAIM Math. Model. Numer. Anal.*, vol. 3, pp. 35–43, 1969.
- [19] R. Fletcher and C. M. Reeves, “Function minimization by conjugate gradients,” *Comput. J.*, vol. 7, pp. 149–154, 1964.
- [20] Y.-H. Dai and Y. Yuan, “A nonlinear conjugate gradient method with a strong global convergence property,” *SIAM J. Optim.*, vol. 10, pp. 177–182, 1999.
- [21] M. Schuld, V. Bergholm, C. Gogolin, J. Izaac, and N. Killoran, “Evaluating analytic gradients on quantum hardware,” *Phys. Rev. A* 99, 032331 (2019). <https://doi.org/10.1103/PhysRevA.99.032331>

- [22] A. Mari, T. R. Bromley, and N. Killoran, “Estimating the gradient and higher-order derivatives on quantum hardware,” *Phys. Rev. A* 103, 012405 (2021). <https://doi.org/10.1103/PhysRevA.103.012405>
- [23] D. Wierichs, J. Izaac, C. Wang, and C. Yen-Yu Lin, “General parameter-shift rules for quantum gradients,” *Quantum* 6, 677 (2022). <https://doi.org/10.22331/q-2022-03-30-677>.
- [24] V. Bergholm, J. Izaac, M. Schuld, C. Gogolin, S. Ahmed, V. Ajith, M. S. Alam, G. Alonso-Linaje, B. AkashNarayanan, A. Asadi et al., “PennyLane: Automatic differentiation of hybrid quantum-classical computations,” <https://doi.org/10.48550/arXiv.1811.04968>
- [25] T. Akiba, S. Sano, T. Yanase, T. Ohta, and M. Koyama, “Optuna: A Next-generation Hyperparameter Optimization Framework,” 2019. <https://optuna.org>.
- [26] A. Kandala, A. Mezzacapo, K. Temme, M. Takita, M. Brink, J. M. Chow, and J. M. Gambetta, “Hardware-efficient variational quantum eigensolver for small molecules and quantum magnets,” *Nature* 549, 242-246 (2017). <https://doi.org/10.1038/nature23879>.